Numerical Investigation Of Effect Of Fuel Jet Configuration On Scramjet Combustor Performance

Akshat Deshpande, Girish Barpande

Abstract: Recently few countries have tested the scramjet engine for aerospace application. The challenge was to achieve complete combustion at supersonic flow and to generate the required thrust for given inlet flow conditions. Research is still going on so as to attain the necessary mixing and efficient combustion inside a scramjet combustor. Performance parameter like total pressure loss across the scramjet combustor is one of the crucial parameters and has to be minimized. Factors such as equivalence ratio, inlet flow conditions affect the combustion process and hence the useful thrust. Also, the fuel injection configuration plays a vital role in mixing and thus on the performance of a scramjet combustor. Over the recent years numerical simulation has been acknowledged as a promising tool for investigation of Scramjet flow. In this work, the investigation of effect of injector configuration has been carried out using a commercial CFD tool. Validation of initial numerical results is done with existing experimental results in the available literature. Modified configurations were obtained by varying number of injection holes for same equivalence ratio. These cases were simulated to observe the right bargain between combustion efficiency and total pressure loss. Conclusions are based on performance parameters like total pressure loss, combustion efficiency, top wall static pressure etc. Mass fraction contour plots of species are obtained to comment further on mixing and combustion performance.

Keywords: Combustion, equivalence ratio, fuel, injector, mixing, pressure, scramjet.

1 INTRODUCTION

The supersonic combustion ramjet (scramjet) engines are a type of air breathing jet engines which utilize atmospheric oxygen in its combustor. Unlike conventional rockets those carry their own oxidizer these engines carry the fuel on board, and obtain the oxidizer by the ingestion of atmospheric oxygen. This requirement limits scramjets to suborbital atmospheric propulsion, where the oxygen content of the air is sufficient to maintain combustion. Scramjets are designed to operate in the hypersonic flight regime, beyond the reach of turbojet engines, and, along with ramjets, fill the gap between the high efficiency of turbojets and the high speed of rocket engines. Fig.1 shows the schematic view of scramjet engine with major components like inlet, isolator, combustor and nozzle. The shock waves present in the converging inlet section compresses the incoming air and decelerates it. An isolator is included between inlet and the combustion chamber so as to avoid the precombustion shock waves entering from inlet to the combustion chamber. It is also used to improve the homogeneity of the flow in the combustor. A constant cross section combustor is used where the gaseous fuel is burnt with atmospheric oxygen to produce heat. In the diverging nozzle the heated products formed due to combustion are accelerated to produce thrust.

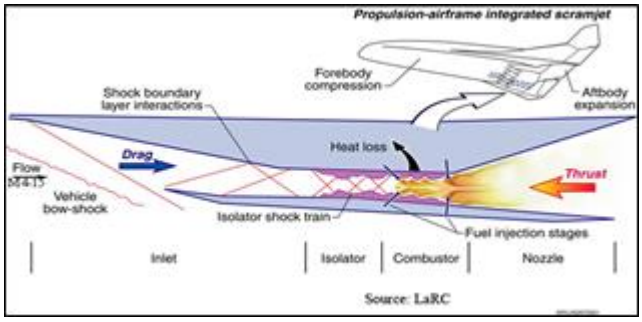

Fig.1 *Schematic view of scramjet engine - Source: NASA Langley*

All these components play a major role in combustion and mixing. Various authors have done research in scramjet field specially in combustion and mixing. M. J. Candon et.al [1] has worked on design optimization of a strut fuel injection-based scramjet engine with the objective of maximizing the thrust. M. J. Candon has found that thrust is largely affected by aerodynamic and combustion effects. Obula Reddy Kummitha et.al [2] has carried out CFD simulations in a scramjet combustor with Mach 2 with use of innovative fuel injection techniques. From the numerical simulation, the author has found that better mixing and combustion efficiency is obtained with the help of strut side fuel injection technique. Rahul Kumar Soni et.al [3] has done work on various injector configurations like straight strut and tapered strut with fixed ramp angle and studied their effects of mixing. Rahul Kumar Soni has found that straight strut gives better performance and is found to be optimum one with better mixing.Gautam Choubey et.al [4] has used three strut fuel injectors namely two side wedge strut and central wedge strut in his work to study their effects on mixing and combustion. From the numerical simulation Gautam Choubey has found that multi strut injection improved the turbulent mixing and the combustion process. K. M. Pandey et.al [5]has a presented a review paper on recent advances in scramjet fuel injection. K. M. Pandey has basically studied different fuel injection schemes and explained their importance

- *Akshat N. Deshpande is a post-graduate student in Design engineering in School of Mechanical Engineering from MIT-World Peace University, Pune, Maharashtra, India.*
- *Prof. Girish Barpande is an Associate Professor, School of Mechanical Engineering, MIT-World peace University, Pune, Maharashtra, India.*

on mixing, combustion and thrust formation. Sadatake Tomioka et.al [6] has carried out experimental work on a staged supersonic combustor with a strut. Here air with Mach 2.5 is used as inlet with hydrogen as a fuel. Experimental results are obtained with only air, air+hydrogen with equivalence ratios of 0.34 and 0.52. Finally, top wall static pressure is plotted for above cases against the combustor length. S. Ramkumar et.al [7] has performed the analysis of scramjet engine with and without strut. Major focus is given to flame holding and its stabilization. The strut is designed using Gambit and analysis is performed using Fluent. Analysis is done with and without hydrogen injection and reults are obtained which concludes that autoignition occurs beyond the strut.Finally the combustion effeciency is also determined.Gautam Choubey et.al [8]has worked on effect of different strut and wall injection techniques on the performance of two strut scramjet combustor. Fluent is used for analysis. It is found that strut+wall1+wall2 injection shows higher mixing compared to other injection techniques. L. Abu-Farah et.al [9] has carried out numerical simulation of single and multi-staged injection of hydrogen in a scramjet combustor. From the simulations it is clear that multi stage injection of H_2 increases the H_2/air mixing by forming vortices and additional shock waves.Juntao Chang et.al [10] has done review on research progress in strut equipped supersonic combustors. Juntao Chang has studied the various phenomenon occurring during combustion, mixing, equivalence ratio and their effects on the flow. Finally, Juntao Chang has given guidelines for the optimization and performance enhancement of the strut-equipped combustor. Bhargav.A et.al [11] has done computational study on effects of shockwave on combustion by predicting shock waves through CFD which in turn affects the combustion efficiency. Finally, through numerical simulation it is observed that shock wave impingement increases the combustion as well as mixing efficiency. Gautam Choubey et.al [12] has done research on effect of different wall injection schemes on flow field of hydrogen fuelled strut-based scramjet combustor. From the numerical simulation, it is found that combined effect of multi strut along with two wall injector improves the efficiency of scramjet compared to multi-strut + wall injection scheme. Gautam Choubey et.al [13]in his work has done research on parametric variation of strut layout and position on the performance of two strut-based scramjet combustor. From the numerical simulation it is observed that the presence of two struts improves the mixing and combustion efficiency of the scramjet when compared to single strut configuration. Yancheng You et.al [14] has worked on injection and mixing inside a scramjet combustor using DES and RANS method. Using these methods in the simulation it was found that flow features as well as the shock waves were captured more precisely. The formation of boundary layers and mixing layers can also be seen clearly through these studies. K. Kumaran et.al [15]has described in his work about the effect of chemistry models on numerical predictions of supersonic combustion of hydrogen. From the simulations it is observed that, multistep chemistry model predicts more higher intricate details of the combustion process and also the wide spread heat release when compared to single step chemistry model. But it is observed that single step chemistry model is capable of predicting the overall performance with considerably less computational cost. Chenlin Zhang et.al [16] has worked on the determining the effect of Mach number and equivalence ratio on scramjet combustor in his experimental work. It has been found that, different equivalence ratios have significant effect on pressure variation in the inlet section of isolator using pressure slopes. Also, the effect of different Mach numbers from the incoming flow at the inlet on the pressure is observed through the slopes of pressure obtained. Y. S. Chen et.al [17]has done numerical study on the effect of mixing on the scramjet combustion and its effectiveness. It has been found that by the use of flame holding hydrogen, mixing of air and fuel is enhanced. This resulted in good combustion efficiency and improved thrust performance. Nobuo Chinzei et.al [18]has worked on the effect of injector geometry on scramjet combustor performance. Through the experiment Nobuo Chinzei found that injector model with shortest constant area section provided better results in terms of peak pressure and combustion efficiency. This area section also provided better mixing between air and fuel and hence increased mixing efficiency.

2 METHODOLOGY

i. Simulations are done for two cases. They are cold flow case and combustion case.
ii. First the cold flow simulation case is carried out.
iii. In this case, initially mesh independent study is performed.
iv. Results are obtained for top wall static pressure for which validation is done with experimental [6] results.
v. Combustion case with parameters as given in the experiment was simulated and validated.
vi. Three different fuel jet configurations were considered here. They are 10 holes, 8 holes and 6 holes respectively for fuel injection. Sonic injection by varying the injection jet diameter for these cases is considered for the same equivalence ratio in all cases.
vii. Performance parameters like total pressure loss, combustion efficiency, top wall static pressure is obtained through simulation for all the three cases and validation of topwall static pressure is done with the experimental [6] results for 10 holes case.
viii. Mass fraction contours of species are obtained for all three configurations from which the combustion and mixing efficiencies are calculated and suitable comments are made.

3 MODELING

3.1 Geometry details

The experimental model of scramjet used by S. Tomioka [6] is shown in fig.2 below. It has got all the geometry features that a typical scramjet combustor consists. The essential components of scramjet engine with their dimensions are described in the geometry here. An intrusive strut type fuel injector is used.

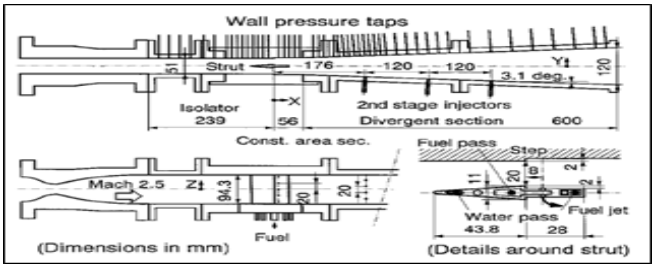

Fig.2 *Scramjet Geometry (S. Tomioka) [6]*

In this research work the same geometry is modeled using CATIA V5 software. The front and isometric views of the model are shown in Fig.2 and Fig.3 respectively.

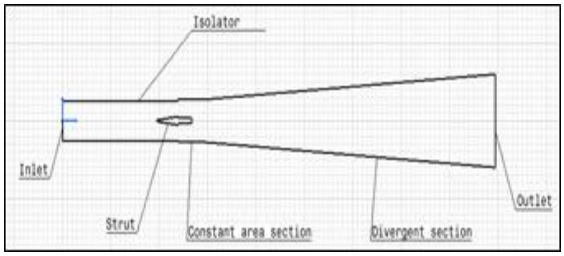

Fig.3 *Line diagram of combustor model*

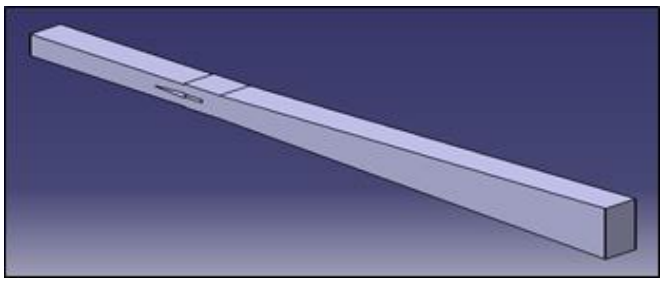

Fig.4 *Isometric view of combustor model*

4 MESHING

4.1 Mesh details

The software used for meshing and analysis is STAR-CCM+13.02. Since there is only one body, region-based meshing approach is used along with the inbuilt mesh models there in the software. The region near the step is very critical due to the steep flow gradients and shock boundary layer interactions. Hence refinement with the prism layer is done so as to capture the flow physics near the complete strut. Number of cells created after meshing are 22,54,678 cells.

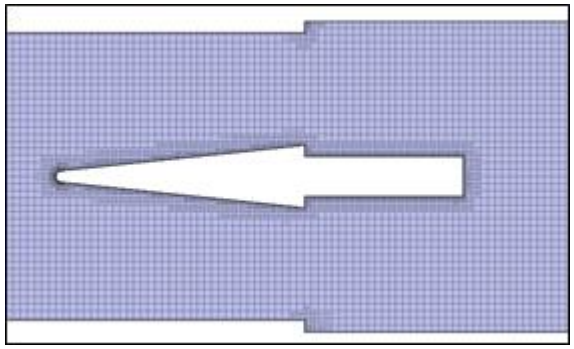

Fig.5 *Trimmed Mesh (Hex Mesh)*

4.2 Mesh model reference values

Base size:	0.5mm
Maximum Cell Size:	250.0% of base
Number of Prism Layers:	2
Prism Layer Stretching:	1.5
Prism Layer Thickness:	33.33 % of base
Surface Growth Rate:	1.3
Surface Size: Relative Minimum Size:	25.0 % of base
Relative Target Size:	250.0% of base

4.3 Mesh values of Refinement region (Strut region)

Surface Size: Relative Minimum Size:	15.0 % of base
Relative Target Size:	80.0 % of base

5 GOVERNING EQUATIONS

Following are the governing equations used for the simulations. By putting the initial and boundary conditions, the equations are solved using mainly coupled solver incorporated in the chosen commercial software and the results are obtained.

1. Continuity equation

$$\frac{\partial}{\partial t}\int_V \rho dV + \oint_A \rho \mathbf{v}\cdot \mathrm{d}\mathbf{a} = \int_V S_u dV \quad (1)$$

2. Momentum equation

$$\frac{\partial}{\partial t}\int_V \rho \mathbf{v} dV + \oint_A \rho \mathbf{v}\otimes\mathbf{v}\cdot d\mathbf{a} = -\oint_A p\mathbf{I}\cdot d\mathbf{a} + \int_A \mathbf{T}\cdot \boldsymbol{d}\mathbf{a} + \int_V \mathbf{f_b} dV \quad (2)$$

3. Energy equation

$$\frac{\partial}{\partial t}\int_V \rho E dV + \oint_A \rho H\mathbf{v}\cdot d\mathbf{a} = -\oint_A \dot{\mathbf{q}}''\cdot d\mathbf{a} + \oint_A \mathbf{T}\cdot\mathbf{v}\, d\mathbf{a} + \int_V \mathbf{f_b}\cdot\mathbf{v}\, dV + \int_V S_E dV \quad (3)$$

Additionally, conservation equations for species mass fractions (Y_i) are solved.

$$\frac{\partial}{\partial t}\left(\int_{\tilde{V}} \rho Y_i\right) d\tilde{V} + \oint_A \rho Y_i(\mathbf{v}-\mathbf{v_g})\cdot d\tilde{\boldsymbol{a}} = \oint_A \left[J_i + \frac{\mu_t}{\sigma_t}\nabla Y_i\right] d\mathbf{a} + \int_{\tilde{V}} S_{Y_i} d\tilde{V} \quad (4)$$

6 INITIAL AND BOUNDARY CONDITIONS

Knudsen number is used in CFD to verify whether CFD is valid to carryout numerical simulation or not. It is given by, where M=2.5, R_e= 1.1×10^7 and γ = 1.4.

Knudsen number $K_n = \frac{M}{R_e}\times\sqrt{\frac{\gamma\times\pi}{2}}$ (5)

substituting the values in above equation we get,

K_n = 3.37032×10^{-7}

As K_n is less than 0.01, hence CFD is valid.

6.1 Air Inlet conditions

Following are the air inlet conditions corresponding to those given in the experiment ref (S. Tomioka) [6]. These are also the inlet conditions for a typical scramjet flight of Mach 7.

P_t = 1×10^6 Pa, M = 2.5, γ = 1.4, T_t = 1550K, R_e = 1.1×10^7

C_p= 1kJ/kg.K, C_v =0.718kJ/kg.K Ideal gas, steady compressible flow is assumed here.

6.2 Calculations of boundary values

Following are the calculations [19],[20] performed to obtain inlet boundary conditions for the given air inlet conditions. To calculate Static temperature T, we have,

$$\frac{T_t}{T} = 1 + \frac{\gamma-1}{2}\times M^2 \quad (6)$$

Substituting the values in above equation we get,

Static temperature obtained was, T= 666.66 K

Velocity of sound in air, $a = \sqrt{\gamma \times R \times T}$ (7)

substituting the values in above equation we get,

a = 517.54m/s

Mach number, $M = \frac{V}{a}$ (8)

substituting the values in above equation we get,

Velocity of body in air, V = 1293.85 m/s

To calculate static pressure, we have,

$$\frac{P_t}{P} = \left(1 + \frac{\gamma-1}{2} \times M^2\right)^{\frac{\gamma}{\gamma-1}} \quad (9)$$

substituting the values in above equation we get,

static pressure, P = 58530.87Pa

To calculate density ρ, we have,

$$a = \sqrt{\gamma \times R \times T}$$

$$a = \sqrt{\gamma \times \frac{P}{\rho}} \quad (10)$$

substituting the values in above equation we get,

Density of air, ρ = 0.3059kg/m^3

Inlet area as per geometry, A = 47.15mm×51mm

= 2404.65mm^2

Mass flow rate, $\dot{m} = \rho \times A \times V$ (11)

substituting the values in above equation we get,

$\dot{m}$ = 0.95173kg/s

To calculate Supersonic static pressure P_{ss}, we have,

$$\frac{P_{ss}}{P_t} = \left(1 + \frac{\gamma-1}{2} \times M^2\right)^{\frac{-\gamma}{\gamma-1}} \quad (12)$$

substituting the values in above equation we get,

P_{ss} = 58527.663 Pa

But as Ps is lesser than atmospheric pressure, it will become

P_{ss} = 58527.663-101325

P_{ss} = -42797.337 Pa

7 SIMULATION OF COLD FLOW CASE

7.1 Mesh independent study

The mesh used is hex mesh which resembles the shape of a block. The mesh size is described in terms of base size. Where the generated mesh is proportional to the base size. The base sizes used here are: 0.75mm, 0.55m and 0.5mm respectively. Simulation is performed for each base size mesh and results are obtained. The best mesh size is selected after observing the contours of Mach number, Velocity and top-wall static pressure plot. Comparison of results is done and is shown in the Table I. The % of average value of error of numerical top-wall static pressure with the experimental values is obtained with all the three meshes and is shown Table II respectively. Mesh size is selected based on the % error value.

7.2 Cold flow results

The residual plot indicate that the solution is converged with convergence criteria for continuity, X-momentum, Y-momentum, Z-momentum and Energy as 10^{-3}.For turbulent dissipation rate and turbulent kinetic energy, the convergence criteria is 10^{-10} and 10^{-13} respectively. Following are the various plots and contours obtained after simulation of cold flow case

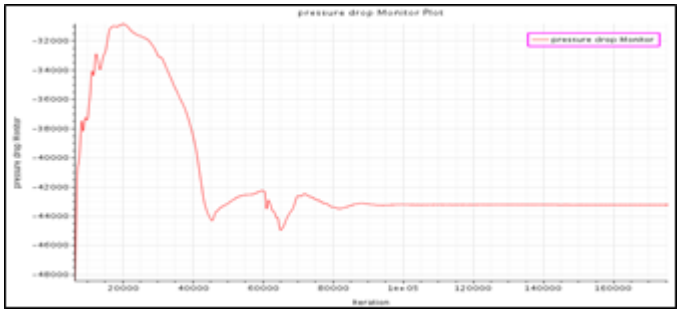

Fig.6 *Pressure drop monitor plot for cold flow case*

Fig.7 *Validation of Top wall static pressure vs length of combustor Experimental_st_Pr (S. Tomioka) [6]*

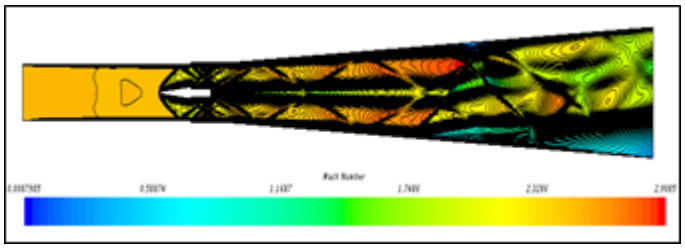

Fig.8 *Mach number contour (make it visible zoom)*

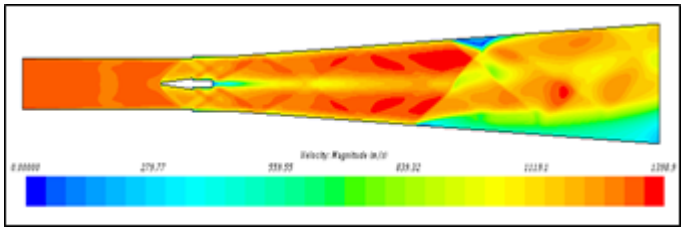

Fig.9 *Velocity contour*

TABLE I

Comparison of Results between Three Different Meshes Obtained by Using Segregated Flow Solver

Base size(mm)	Topwall static pressure (Pa) max	Velocity(m/s) max	Mach number(max)
0.75	151697	1413.4	2.9983
0.55	152975	1395.8	2.8892
0.5	148751	1398.8	2.9062

TABLE II

Percentage error for Top Wall Static Pressure when compared with Experimental Results for different Mesh sizes.

Base size in mm	*Average % error*
0.75	*27.50998*
0.55	*22.99874*
0.50	*21.59527*

7.3 Discussion

i. Table I shows the comparison of results between three different meshes obtained by using segregated flow solver. From the table we can see that the magnitude of velocity, topwall static pressure and the Mach number are nearly the same. Hence mesh independent study is performed and is found to be true.

ii. Table II shows the comparison of results of top wall static pressure obtained with mesh of base size 0.75mm, 0.55mm, 0.5mm with experimental results. The % average value of error of the topwall static pressure with the experimental results is calculated and is found that the error is minimum for the mesh with base size 0.5mm. Hence mesh with base size 0.5mm is selected for further simulation.

iii. The simulation results of topwall static pressure are validated with the experimental values as shown in Fig.7. There is a discontinuity in simulation curve due to two different line probes which are separated by the step on the top wall and not having common X co-ordinate.

iv. From the Mach number contour Fig.8, the shock waves can be captured more easily. We can see that the bow shock is created at the strut nose, the shock train is formed at the downstream of the step with the flow separation occurring in the divergent section near the walls which is seen in blue colour in the contour.

v. Fig.9 shows the velocity contour. It indicates that the velocity is decreasing in the divergent section due to flow separation and hence there is a pressure rise seen.

vi. The pressure drop monitor plot as shown in Fig.6 is obtained by generating reports for surface average pressure at inlet and surface average pressure at outlet and then subtracting it using the field functions by creating plane sections at inlet and outlet faces. From the above plot we can say that the solution is converged because pressure drop curve becomes a straight line after 80000 iterations. If we continue the iterations also, the curve remains straight. Hence, we can stop the run, since the solution has converged. Steady state is achieved here.

8 COMBUSTION CASE

8.1 Combustion scheme

Here hydrogen gas (H_2) is used as fuel along with air. Hydrogen is injected at sonic speed. Equivalence ratio of 0.34 is used from which the mass flow rate is calculated. Standard Eddy break up (EBU) model is used as chemistry model which is a type of reacting species transport model used for combustion of multi component gas here. The global one step reaction mechanism is used which is:

$$2H_2 + O_2 \rightarrow 2H_2O.$$

8.2 10-hole jet configuration

8.2.1 Geometry details

As shown in the figure below, injection holes are created inside the strut. There are total 10 injection holes. But as the geometry is symmetric, only 5 holes are shown.

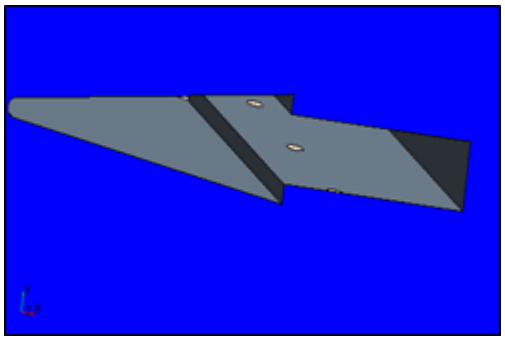

Fig.10 *Isometric view of strut*

8.3 Meshing

8.3.1 Mesh details

Meshing for the combustion case is performed by using the following mesh models: Surface remesher, extruder, prism layer mesher and trimmer (hexahedral mesher). Number of cells created after meshing are 795164 cells. Mesh with base size 0.5mm is used and the mesh parameters like maximum cell size, number of prism layers, surface size etc. are defined for strut region to capture the shock waves. The mesh around the strut is shown in the figure below.

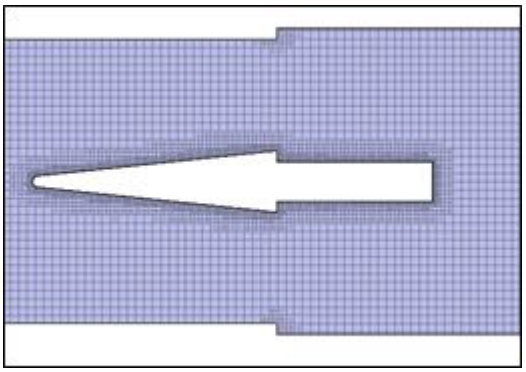

Fig.11 *Trimmed Mesh (Hex Mesh)*

8.4 Initial and boundary conditions

8.4.1 Fuel Inlet conditions

Following are the hydrogen inlet conditions corresponding to those given in the experiment ref (S. Tomioka) [6].

ϕ=0.34,$(F/A)_{st}$=0.0291,γ=1.40944,T=303K, R=4.157KJ/KgK

C_p = 14.32kJ/kg.K, C_v = 10.16kJ/kg.K, d= 2.5mm

The species mass fraction constituents used at the air inlet are: O_2 = 0.139, H_2O = 0.198, N_2 = 0.663. The species mass fraction of constituents used at fuel inlet is H_2 =1. Ideal gas, steady compressible flow is assumed here. Coupled flow solver is used.

8.4.2 Calculations of boundary values

Following are the calculations performed to obtain the fuel boundary conditions from the given fuel inlet conditions.

Equivalence ratio, $\phi = \frac{\frac{\dot{m}_{H_2}}{mass\ of\ air}}{(F/A)st}$ (13)

$$0.34 = \frac{\frac{\dot{m}_{H_2}}{2\times 0.95173}}{0.0291}$$

$\dot{m}_{H_2}$ = 0.01883kg/s for all 10 injectors in total.

Mass flow rate per injector = $\frac{0.01883}{10}$ = 0.001883kg/s

Velocity of sound in air, $a = \sqrt{\gamma \times R \times T}$

substituting the values in above equation we get,

a = 1332.399 m/s

As injection is at sonic speed, therefore V=a=1332.399 m/s

Diameter of jet, d = 2.5mm

Area of fuel injector, $A_f = \frac{\pi}{4} \times d^2$ (14)

substituting the values in above equation we get,

A_f = 4.90873× 10^{-6}mm^2

$\dot{m}_{H_2}$= ρ×A×V

0.001883 = ρ×4.90873× 10^{-6} × 1332.399

Density of H_2, ρ = 0.28790 kg/m^3

Static Pressure, $P = \frac{\dot{m}_{H_2} RT}{AV}$ (15)

substituting the values in above equation we get,

P =362634.8431Pa

Total Pressure, $P_t = P + \frac{\rho V^2}{2}$ (16)

substituting the values in above equation we get,

P_t = 617388.5413Pa

To calculate Supersonic static pressure P_{ss}, we have

$$\frac{P_{ss}}{P_t} = \left(1 + \frac{\gamma - 1}{2} \times M^2\right)^{\frac{-\gamma}{\gamma - 1}}$$

substituting the values in above equation we get,

P_{ss}=325176.68Pa

To calculate Total temperature T_t, we have,

$$\frac{T}{T_t} = \left(1 + \frac{\gamma - 1}{2} \times M^2\right)^{-1}$$

substituting the values in above equation we get,

T_t = 365.03K

Similarly, the calculation is carried out of for 6- and 8-holes configuration. The total mass flow rate is kept constant and is divided by the number of holes to get mass flow rate through single hole. $\dot{m}_{H_2}$= ρ×A×V, this equation is used to find the diameter of jet diameter, by knowing all other terms in the equation. From this information we can find static pressure, total pressure, supersonic static pressure and total temperature. The simulations are performed for these two cases of new jet configurations.

8.5 8-hole jet configuration

8.5.1 Geometry details

There are total 8 injection holes. But as the geometry is symmetric, only 4 holes are shown.

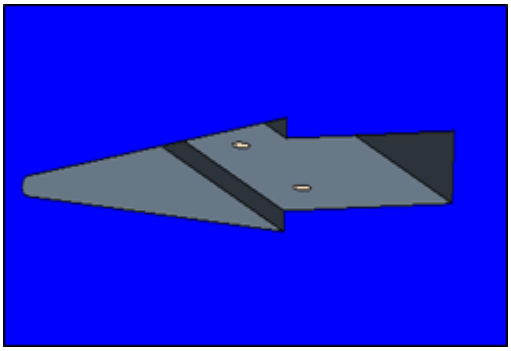

Fig.12 *Isometric view of strut*

Diameter of each jet, d = 2.7950mm

Mass flow rate/injector, $\dot{m}_{H_2}$= 0.00235375kg/s

The base size of the mesh 0.5mm is kept same for meshing of the geometry for all the fuel injector configurations. Only the mesh parameters are varied near the strut region for refinement and to achieve accurate results.

8.6 Meshing

8.6.1 Mesh details

Number of cells created after meshing are 103446 cells. The mesh generated is as shown in the figure below.

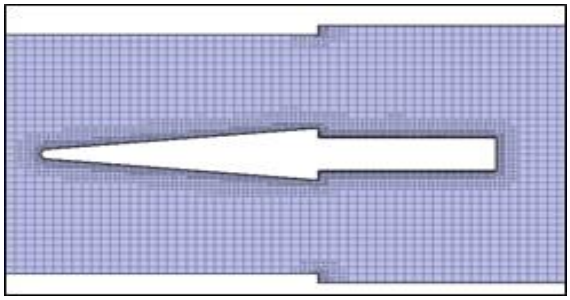

Fig.13 *Trimmed Mesh (Hex Mesh)*

8.7 6-hole jet configuration

8.7.1 Geometry details

There are total 6 injection holes. But as the geometry is symmetric, only 3 holes are shown.

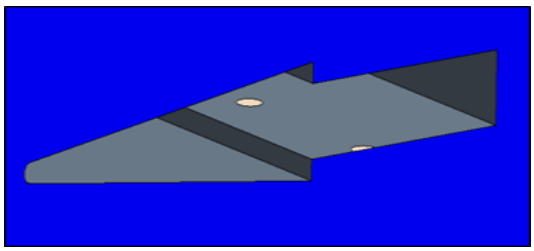

Fig.14 *Isometric view of strut*

Diameter of each jet, d = 3.2273mm

Mass flow rate/injector, $\dot{m}_{H_2}$ = 0.003138kg/s

8.8 Meshing

8.8.1 Mesh details

Number of cells created after meshing are 795072 cells. The mesh generated is as shown in the figure below.

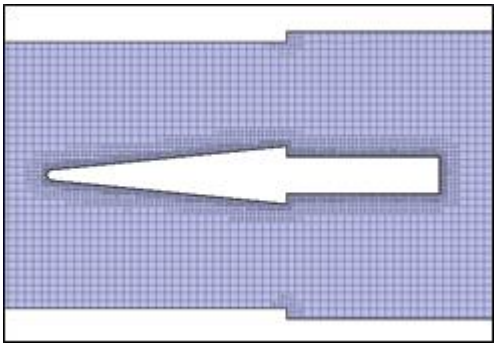

Fig.15 *Trimmed Mesh (Hex Mesh)*

9 RESULTS AND DISCUSSION OF COMBUSTION CASE

9.1 Results of 10-hole jet configuration

Following are the various plots and contours obtained after simulation of combustion case of 10 injection holes.

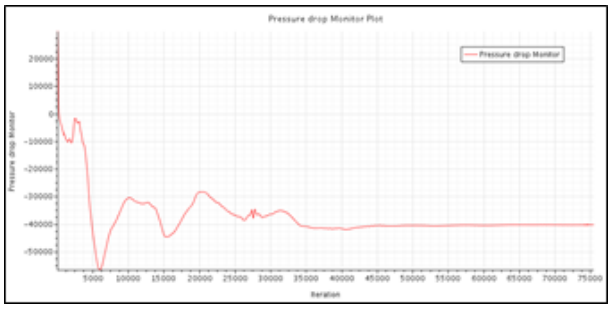

Fig.16 *Pressure drop monitor plot*

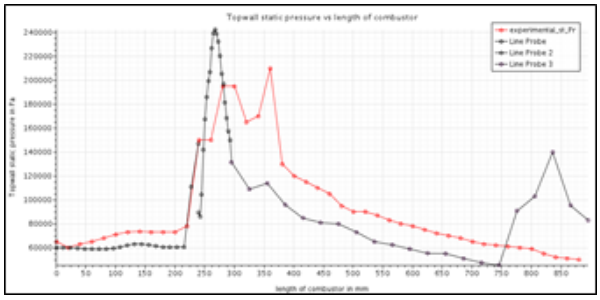

Fig.17 *Validation of Top wall static pressure vs length of combustor Experimental_st_Pr (S. Tomioka) [6] for 10-hole fuel injector configuration*

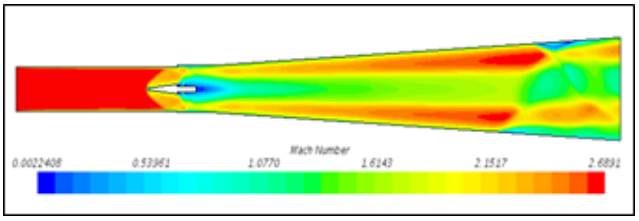

Fig.18 *Mach number contour*

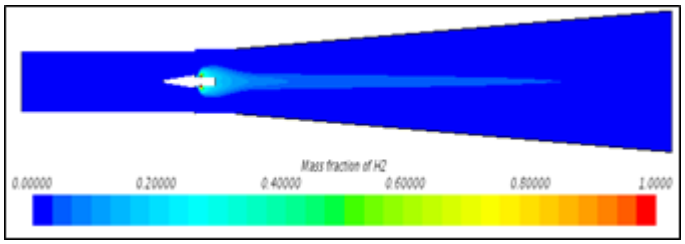

Fig.19 *H_2 Mass fraction contour on symmetric plane*

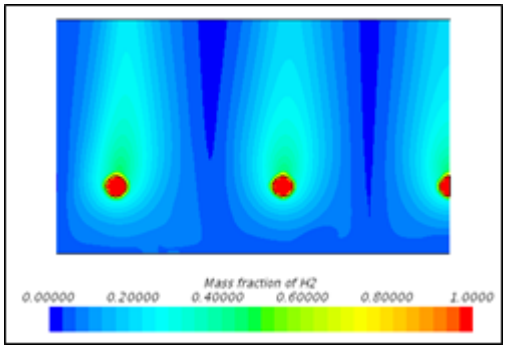

Fig.20 *H_2 Mass fraction contour on injection side*

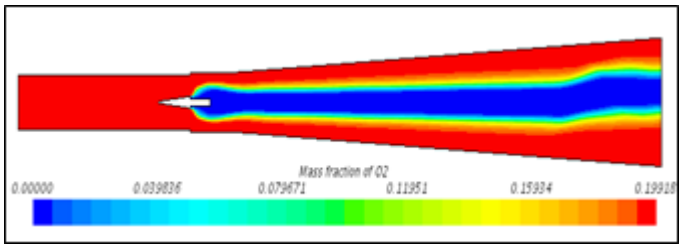

Fig.21 *O_2 Mass fraction contour*

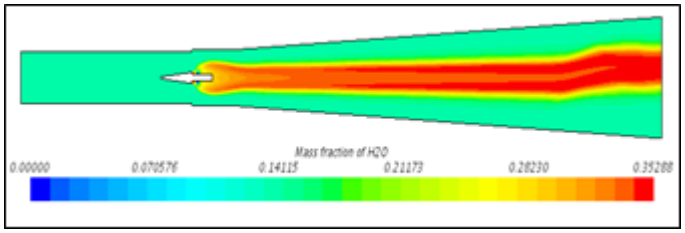

Fig.22 *H_2O Mass fraction contour*

9.2 Results of 8-hole jet configuration

Following are the various plots and contours obtained after simulation of combustion case of 8 injection holes.

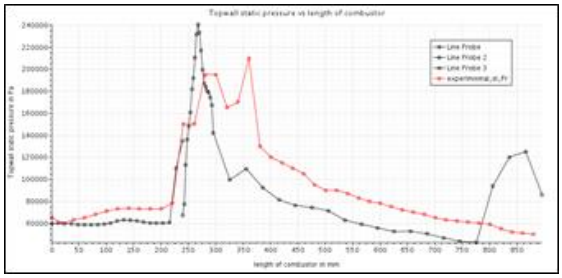

Fig.23 *Top wall static pressure vs length of combustor Experimental_st_Pr (S. Tomioka) [6] for 8-hole fuel injector configuration*

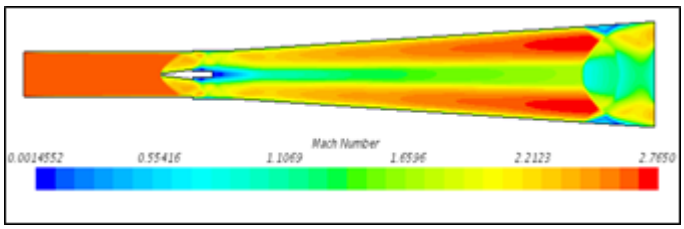

Fig.24 *Mach number contour*

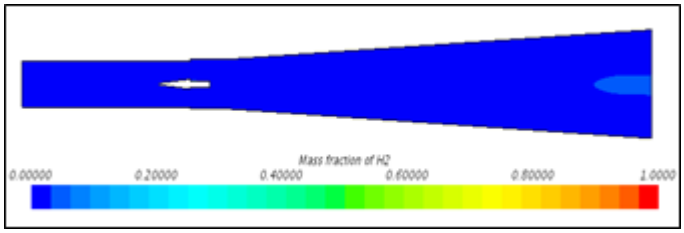

Fig.25 *H_2 Mass fraction contour on symmetric plane*

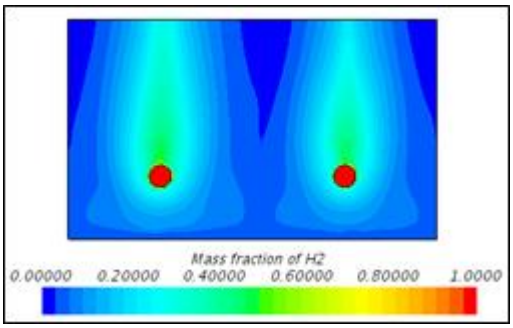

Fig.26 *H_2 Mass fraction contour on injection side*

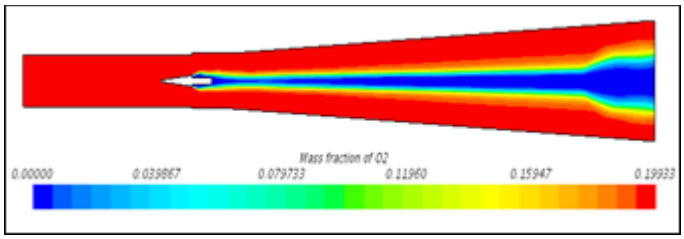

Fig.27 *O_2 Mass fraction contour*

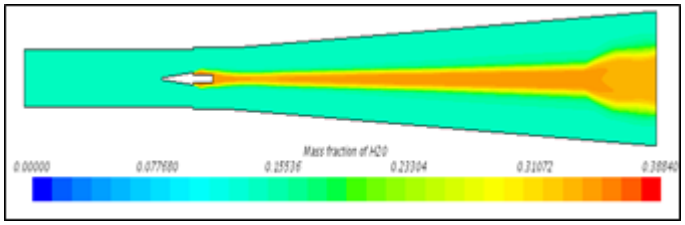

Fig.28 *H_2O Mass fraction contour*

9.3 Results of 6-hole jet configuration

Following are the various plots and contours obtained after simulation of combustion case of 6 injection holes.

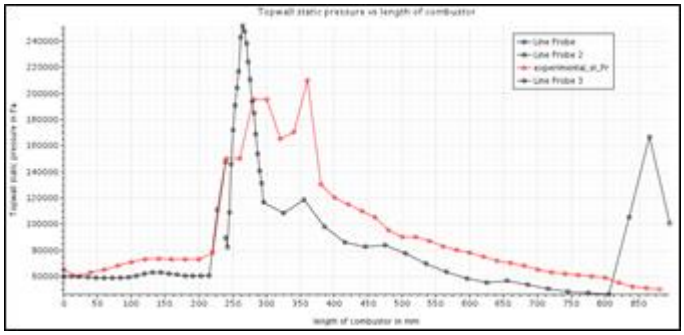

Fig.29 *Top wall static pressure vs length of combustor Experimental_st_Pr (S. Tomioka) [6] for 6-hole fuel injector configuration*

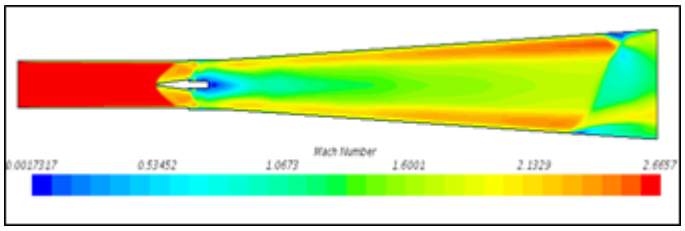

Fig.30 *Mach number contour*

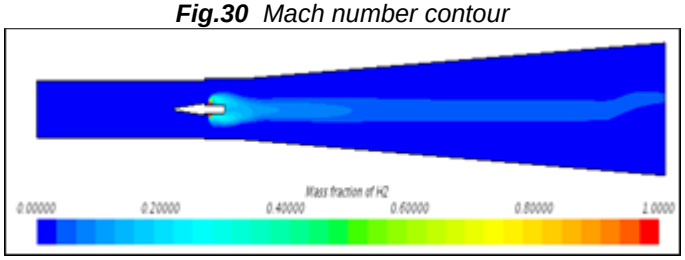

Fig.31 *H_2 Mass fraction contour on symmetric plane*

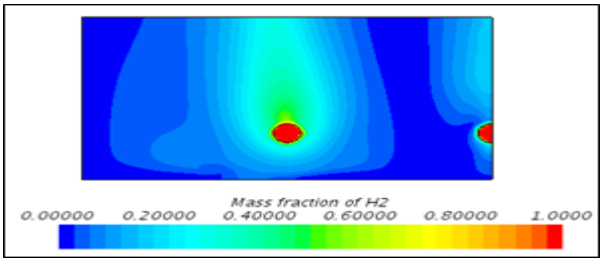

Fig.32 *H_2 Mass fraction contour on injection side*

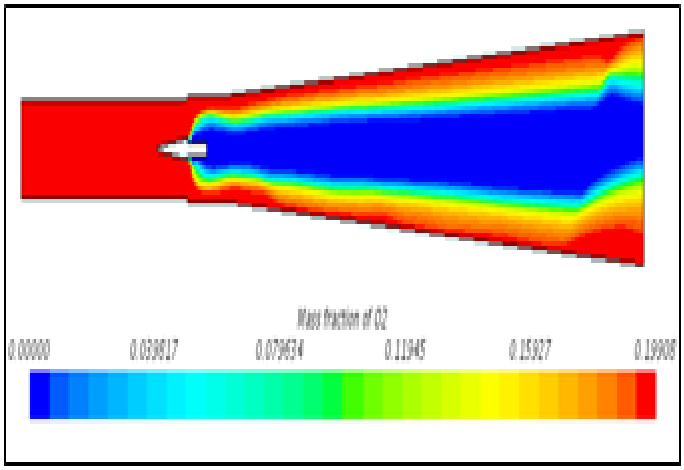

Fig.33 *O_2 Mass fraction contour*

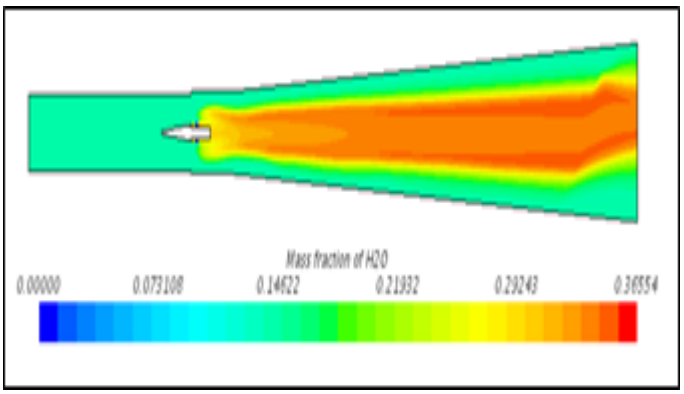

Fig.34 *H_2O Mass fraction contour*

Following are the equations used to calculate combustion and mixing efficiency. They are:

Combustion Efficiency, $\eta_c = \frac{\dot{m}_{H_{2,inj}} - \dot{m}_{H_{2,out}}}{\dot{m}_{H_{2,inj}}}$ (17)

Mixing Efficiency, $\eta_{mix} = \frac{\dot{m}_{H_{2,inj}} - \dot{m}_{H_2O,out}}{\dot{m}_{H_{2,inj}}}$ (18)

TABLE III

Combustion and mixing efficiencies for different injector configurations

Injector configuration	*Combustion efficiency*	*Mixing efficiency*
10 holes	*83.95%*	*80.72%*
8 holes	*76.91%*	*80.50%*
6 holes	*83.47%*	*80.94%*

11 CONCLUSION

i. From the results and discussion of mesh independent study in cold flow case, it is clear that mesh with base size 0.5mm is appropriate for further simulation.

ii. Pressure drop monitor plot in cold flow case, indicates that a fair and converged solution has been obtained.

iii. From the Mach number and velocity contours in cold flow case, the nature of shock structure inside the combustor is clearly revealed. However a flow separation is also seen in the divergent section.

iv. The cold flow case is validated with topwall static pressure by comparing it to the experimental top wall static pressure values and is found to be closely matching with the experimental curve.

v. The combustion case with equivalence ratio of 0.34 for 10 injection holes is validated for topwall static pressure with the available experimental top wall static pressure and is found that the simulation curve lags in the pressure rise especially in the divergent section of the combustor. However the average peak pressure inside the constant area region can be said to be matching with experimental values.

vi. The reason for a little variation in the static pressure plot at isolator region for both cold flow case and combustion case may be due to the use of facility nozzle at the inlet of isolator during the experimentation.

vii. The contours of Mach number in combustion case, show a reduction in Mach number at the injector region due to the temperature rise of combustion. Also, flow separation is seen to be occurring at the exit in the divergent section.

viii. From the hydrogen mass fraction contour, we can see that H_2 concentration is higher at the injection side inside the strut and decreases gradually from the strut till the end of combustor. This indicates that there is gradually burning or mixing that is taking place in the divergent section.

ix. From the O_2 mass fraction contour, it can be seen that the core region is less with oxygen when compared to top and bottom regions of the core flow. This is indicating the consumptions of O_2 near the core region only.

x. From the H_2O Mass fraction contour, it can be seen that formation of H_2O is more in the constant area region and it decreases and remains constant along the combustor length. This indicates that H_2O is formed in higher concentration after the reaction in the strut region.

xi. Combustion efficiency is highest for 10 -hole injector configuration which indicates that the maximum amount of hydrogen is consumed in the reaction and very less amount of hydrogen is left unburnt and it is least for 8-hole injector configuration.

xii. Mixing efficiency is highest for 6-hole injector configuration and is least for 8-hole injector configuration indicating formation of H_2O is more in 6-hole case and proper mixing is taking place.

xiii. The total pressure loss is least for 6-hole jet configuration with magnitude of -3.703698×10^4 Pa and also the topwall static pressure is highest for this configuration with a magnitude of 2,51,663Pa which is desired.

12 ACKNOWLEDGEMENT

I would like to express great gratitude to the School of Mechanical Engineering of Maharashtra Institute of Technology World Peace University (MIT WPU), Pune, Maharashtra, India for providing Computational facilities at their CFD Laboratory to carry out the research work. It was extremely helpful for the completion of this work.

REFERENCES

[1] M.J. Candon, H. Ogawa, "Numerical analysis and design optimization of supersonic after- burning with strut fuel injectors for scramjet engines," Science Direct, Acta Astronautica, vol. 147, pp. 281-296, June 2018.

[2] Obula Reddy Kummitha, Lakka Suneetha, K.M. Pandey,"Numerical analysis of scramjet combustor with innovative strut and fuel injection techniques," Science Direct, pp. 1-12, January 2017.

[3] Rahul Kumar Soni, Ashoke De, "Investigation of strut ramp injector in a scramjet combustor:Effect of strut geometry,fuel and jet diameter on mixing characteristics," Journal of Mechanical Science and Technology, vol. 31, no. 3, pp. 1169-1179, 2017.

[4] Gautam Choubey, K. M Pandey, Ambarish Maji, Tuhin Deshmukhya,
Ajoy Debbarma, "Computational investigation of Multi-strut injection of hydrogen in a scramjet combustor," Materials Today:Proceedings 4, p. 2608–2614, 2017.

[5] K.M.Pandey,T. Sivasakthivel, "Recent Advances in Scramjet Fuel Injection - A," International Journal of Chemical Engineering and Applications, vol. 1, no. 4, December 2010.

[6] Sadatake Tomioka, Atsuo Murakami, Kenji Kudo, and Tohru Mitani,"Combustion Tests of a Staged Supersonic Combustor with a Strut," Journal of Propulsion and Power, vol. 17, no. 2, March–April 2001.

[7] S. Ramkumar, M. S. Vijay Amal Raj, Rahul, Mahendra Vaity,"Analysis of Scramjet Engine With And Without Strut," International Journal of Engineering Research & Technology (IJERT), vol. 2, no. 1, January 2013.

[8] Gautam Choubey, K.M. Pandey,"Effect of different strut+wall injection techniques on the performance of two-strut scramjet combustor," ScienceDirect, International journal of hydrogen energy, pp. 1-17, April 2017.

[9] Abu-Farahn, O.J. Haidn, H.-P. Kau,"Numerical simulations of single and multi-staged injection of H2 in a supersonic scramjet combustor," Elsevier, Propulsion and Power Research, vol. 3, no. 4, pp. 175-186, 2014.

[10] Juntao Chang, Junlong Zhang, Wen Bao, Daren Yu,"Research progress on strut-equipped supersonic combustors for scramjet application," Elsevier, Progress in Aerospace Sciences, October 2018.

[11] J. Naidu, Bhargav.A,"Computational Study on Effects of Shockwave on Combustion and Injected Fuel By Unconventional Positioning of Injectors," International Journal of Engineering Science Invention (IJESI), pp. 51-56.

[12] Gautam Choubey, K.M. Pandey,"Effect of different wall injection schemes on the flow-field of hydrogen fuelled strut-based scramjet combustor," Elsevier,Acta Astronautica, vol. 145, pp. 93-104, January 2018.

[13] Gautam Choubey, K.M. Pandey,"Effect of parametric variation of strut layout and position on the performance of a typical two-strut based scramjet combustor," ScienceDirect, International journal of hydrogen energy, pp. 1-16, 2017.

[14] Yancheng You, Heinrich Luedeke, Klaus Hannemann,"Injection and mixing in a scramjet combustor: DES and RANS studies," Science Direct,Proceedings of the Combustion Institute 34, pp. 2083-2092, 2013.

[15] K. Kumaran, V. Babu,"Investigation of the effect of chemistry models on the numerical predictions of the supersonic combustion of hydrogen, Combustion and Flame," Elsevier, Combustion and Flame 156, pp. 826-841, January 2009.

[16] ChenlinZhang, "Effect of Mach number and equivalence ratio on the pressure rising variation during combustion mode transition in a dual-mode combustor," Elsevier, Aerospace Science and Technology, vol. 72, pp. 516-524, 2018.

[17] Y.S. Chen, Y. Y. Liana, T. H. Chou, Alfred Lai, J. S. Wu, "Mixing Effectiveness Study in Scramjet Combustion," ScienceDirect,Procedia Engineering 67, pp. 218-229, 2013.

[18] Nobuo Chinzei, Tomoyuki Komuro, Kenji Kudou, Atsuo Murakami Kouichiro Tani, Goro Masuya and Yoshio Wakamatsu,"Effects of Injector Geometry on Scramjet combustor performance," Journal of propulsion and power, vol. 9, no. 1, Jan.-Feb. 1993.

[19] John D.Anderson,Jr., Fundamentals of Aerodynamics,3rd ed. McGraw
Hill,2001.

[20] Ethirajan Rathakrishnan, Applied Gas Dynamics, Wiley India Pvt.Ltd,
Reprint 2012.

About Authors

Akshat N. Deshpande
He is a post-graduate student in Mechanical Design engineering from MIT-World Peace University, Pune. He Completed his Bachelor's in Mechanical Engineering from KLS Gogte Institute of Technology, Belgaum under Visvesvaraya Technological University, Belgaum, Karnataka. His area of intertest includes Machine design, Tribology,

FEA and CFD.

Prof. Girish S. Barpande
Presently working as an Associate Professor in school of Mechanical Engineering from MIT-World Peace University, Pune. He is currently pursuing Ph.D. in Mechanical engineering from SPPU. His research area includes Tribology, Aerodynamics and CFD. He has 3 research publication in National/International journal. He has a total of 22.5 years of experience with 20 years of teaching experience and 2.5years of industrial experience. He is a member of SAE India and life member of tribology society of India (TSI)